Ground- and excited-state properties of neutral and anionic selenium dimers and trimers

Christoph Heinemann and Wolfram Koch*
Institut für Organische Chemie der Technischen Universität Berlin, Straße des 17. Juni 135, D-10623 Berlin, Germany

Gottlieb-Georg Lindner
Institut für Angewandte Chemie Adlershof, D-12489 Berlin, Germany

Dirk Reinen
Fachbereich Chemie, Philipps-Universität Marburg, D-35032 Marburg, Germany

Per-Olof Widmark
IBM Sweden, P.O. Box 4104, S-220312 Malmö, Sweden
(Received 15 March 1996)

Ab initio molecular-orbital methods using a newly constructed large, flexible basis set of the atomic-natural-orbital type and extensive treatments of electron correlation were used to accurately predict the ground-state potential-energy curves of Se_2 and Se_2^-. In addition, the potential curves of low-lying electronically excited states of the Se_2^- anion, which are coupled to the ground state through the electronic dipole operator, are determined. Calibration of the accuracy expected for the employed theoretical models is achieved by calculations on electronically excited states of neutral Se_2, for which accurate experimental data are available. Besides reporting accurate predictions for spectroscopic constants, electron affinities, and transition matrix elements, particular emphasis is laid on the use of the computed dimer potential-energy curves for interpreting the recently investigated peculiar optical properties of diatomic selenium species embedded in solid host matrices. Further, the equilibrium geometries and relative stabilities of the C_{2v} and D_{3h} forms of the neutral Se_3 cluster, the electron affinity of Se_3, and the low-lying electronic states of Se_3^- have been investigated theoretically. [S1050-2947(96)06509-2]

PACS number(s): 31.15.Ar, 31.50.+w, 32.10.Hq, 32.70.Cs

I. INTRODUCTION

Accurate information on the spectroscopic and energetic properties of anions is less straightforward to obtain as compared to their neutral and singly positively charged counterparts [1]. Experimental difficulties may already be encountered in anion generation when the electron affinities of the respective neutral molecules are small. The probability of detachment of the additional electron due to chemical reactions or other sources of energy transfer can obstruct the reliable measurement of ground-state data, and affect the observation of electronically excited states even more. On the other hand, theoretical investigations of anions and in particular the reliable determination of electron affinities (EA's) are traditionally among the most demanding fields in quantum-mechanical *ab initio* calculations: (i) The correlation energy of the anion, with an additional, albeit weakly bound, electron is substantially larger than that of the neutral molecule. (ii) The electron density of anions is usually much more diffuse than that of neutral molecules. As a consequence, sophisticated treatments of the correlation energy combined with one-particle basis sets augmented by diffuse and high angular momentum functions are required for an appropriate description of the extra electron. Hence today's most elaborate methods for the treatments of the one- and n-particle space problems connected with the solution of a many-electron Schrödinger equation are needed if ''chemical accuracy'' (errors <1 kcal/mol$=0.043$ eV$=350$ cm^{-1}), not to mention higher spectroscopic precision (errors in the cm^{-1} regime), is the target [2].

Despite these principal difficulties, interest in small anionic molecular systems has been growing over recent years. Various kinds of anion spectroscopies have undergone fruitful development, now yielding structural and dynamic information, frequently with a high spectroscopy resolution [3]. However, in many cases the information gained in these experiments is not sufficient to provide a consistent interpretation of the underlying physics and theoretical data for ground- and excited-state potential-energy surfaces of the considered species are required. On this general background and with particular reference to studies of optical properties of anionic chalcogenide clusters in solid host matrices [4,5], we have recently performed accurate *ab initio* molecular-orbital calculations on ground and excited states of O_3^- [6], S_2^- [7], and S_3^- [8]. These studies helped to understand Raman [4], luminescence [4], and photoelectron spectroscopic experiments [9] on these species, and suggested the revision of a formerly deduced value [9(e)] for the electron affinity of S_3 [8,9(f)].

In the present work, we present elaborate calculations for low-lying electronic states of the anionic selenium dimer, particularly focusing on equilibrium distances, vibrational frequencies, excitation and binding energies, electron affinities, and transition-dipole matrix elements. Specifically, we consider the full potential-energy curve of the $^2\Pi_g$ Se_2^-

*Author to whom correspondence should be addressed.

 © 1996 The American Physical Society

ground state, those bound low-lying excited doublet states to which this state is connected via electronic dipole-allowed transitions ($^2\Pi_u$, $^2\Delta_u$, and $^2\Sigma_u^{+/-}$), and the lowest excited quartet state $^4\Sigma_u^-$. A calibration of the accuracy that can be expected for the theoretical predictions is achieved by considering spectroscopic properties and of those low-lying states of *neutral* Se_2 for which reliable experimental data are available. The potential-energy curves for Se_2^- will then be used to interpret recent luminescence and Raman spectra of Se_2^- in sodalith cages [4(b),4(c)], which have revealed unprecedented (with respect to the lower homologue S_2^-) optical properties.

In addition to calculations on the neutral and anionic dimers, we also present theoretical data for the selenium atom (electron affinity, dipole polarizability) and the neutral as well as anionic selenium trimers (C_{2v} vs D_{3h} ground-state geometry, adiabatic EA's, and excitation energies to low-lying anion states). While experimentally determined EA's for the Se atom [2.020 69(3) eV [10]] and the Se_2 molecule (1.94 ± 0.07 eV [11]) have been reported, only a lower bound for the EA of Se_3 (>2.2 eV [11]) has been established on the basis of the nonobservation of electron detachment or photodissociation from Se_3^- by 2.54-eV photons. We will compare our computed EA's for Se and Se_2 to the experimental values, and thus derive an estimate of the accuracy of the computed EA for the triatomic selenium cluster.

Earlier theoretical work on small anionic selenium systems is scarce: While there is now abundant information on O_2^- [6,12], O_3^- [13], S_2^- [7] and S_3^- [8,14], we are not aware of earlier studies of Se_2^-, and only two brief reports on Se_3^- are known to us, i.e., the prediction of vertical electron affinities of around 2.00 eV for the C_{2v}-symmetric form of Se_3 by Niessen, Cederbaum, and Tarantelli [15], and a complete-active space self-consistent field calculation of low-lying Se_3^- states by Basch [16], who also predicted an adiabatic electron affinity of 2.1 eV for Se_3 using fourth-order many-body perturbation theory and a double-ζ polarized basis set. In the neutral regime, Se_2 was studied by Balasubramanian [17(a)] and Bhanuprakash, Hirsch, and Buenker [17(b)] using small- to medium-sized configuration-interaction wave functions and including spin-orbit interaction. The larger clusters from Se_3–Se_{10} were studied by density-functional [16,18] molecular dynamics [18(b)] and pseudopotential [19] methods. However, from a quantitative point of view, and compared to modern computational standards, these earlier studies cannot be regarded as sufficiently accurate for a definite answer to the question whether the lowest-energy isomer of Se_3 adopts the form of an open (C_{2v}) or equilateral (D_{3h}) triangle, which needs to be answered before deducing a reliable theoretical estimate for the electron affinity of Se_3.

Besides the prediction of spectroscopic properties for neutral and anionic selenium dimers and trimers, we will also briefly discuss some methodological points which arose during this study. In particular, an atomic natural orbital (ANO) [20] one-particle basis set was developed for selenium, and its suitability for the questions addressed in this study will be evaluated. Further, the influence of relativistic terms in the Hamiltonian (mostly scalar but, for selected purposes, also spin-orbit effects) on the calculated quantities has been assessed. The remainder of the paper is structured as follows: After a short introduction to the computational procedures, we will first discuss properties of the selenium atom (Sec. III A). Then the spectroscopic (Secs. III B and III C) and energetic (Sec. III D) properties of diatomic Se_2 and Se_2^-, transition dipole matrix elements, and radiative lifetimes (Sec. III E), and their implications for spectroscopic experiments on Se_2^- in host matrices (Sec. III F) will be presented. Section (III G) deals with Se_3, and Se_3^-, and is followed by a summary (Sec. III H) of the important conclusions which can be drawn from the present work. For the discussion of energetic quantities, we are using eV and cm^{-1} units where appropriate. The employed conversion factor is 1 eV=8066 cm^{-1}.

II. THEORETICAL METHODS

A. Basis sets

For a reliable prediction of electron affinities and excited-state properties, a large and flexible Gaussian basis set of the atomic natural orbital type [20] has been generated. The starting primitive set used was the $21s16p10d$ set by Partridge [21]. This is a large and flexible primitive set almost reproducing the numeric Hartree-Fock energy for the selenium atom, with a truncation error of only 0.3 mH on the total energy. For a description of angular correlation effects, an even-tempered $3f2g$ set was optimized with respect to the correlation energy of the selenium atom. Further, all shells were augmented with one diffuse function as an even-tempered continuation. They were added to enhance the description of the outer region of the atom primarily for improved polarizability and electron affinity. Thus the final size of the primitive set is $22s17p11d4f3g$.

The contraction is determined from an averaged density matrix. The eigenvectors (''natural orbitals'') of the averaged density matrix are used as contraction coefficients for the contracted basis functions. The selection is made on eigenvalues (''occupation numbers'') with less populated functions that are discarded first [20(b)]. The states included are Se ^3P, Se^- ^2P, Se^+ ^4S and Se ^3P with a weak external electric field applied. The strength of the field was 0.01 a.u. This field is weak enough not to interfere with the ability of the basis set to give large correlation energies at the same time, the polarizability of the atom is well described. The weight of each density matrix is equal on average.

Since calibration studies on the Se atom (see below) indicated the need for higher angular momentum functions, a single h exponent ($\alpha_h=0.45$; for optimization, see below) was added to the $7s6p5d3f2g$ ANO contraction, thus yielding the final basis set for the studies of Se_2 and Se_2^-, which comprises 199 and 100 primitive and contracted functions per selenium atom (spherical harmonic polarization functions, i.e., $5d$, $7f$, $9g$, and $11h$ components were used throughout). Due to hardware limitations, the h function had to be omitted in the calculations of the selenium trimer. To allow for a proper description of core-core and core-valence correlation effects [22], a $3s3pd3f3g$ even-tempered primitive basis set was optimized using a $5s4p3d2f1g$ valence basis set [23]. The optimization criteria was again the correlation energy of the selenium atom [24]. Spin-orbit calculations employed the compact relativistic effective core potential (RECP) of Stevens *et al.* [25] to treat the 28 core

electrons of Se and the associated $(6s6p)/[3s3p]$ valence basis, augmented by two d-type polarization functions with exponents of 0.676 and 0.169 (six Cartesian components each), respectively, to obtain a final set of triple-ζ plus two polarization functions (TZ2P) quality.

B. Wave functions

For most topics addressed here, the multireference configuration interaction (MRCI) method [26] was employed. The wave function Ψ was partitioned in a reference space comprising all configuration state functions (CSFs) which can be constructed from the selenium $4s$ and $4p$ atomic orbitals for a molecular state in a given spin and space symmetry, and the much larger space of external CSFs generated by symmetry-adapted single and double excitations from each reference function into the virtual orbitals. To generate the necessary molecular orbitals, in a first step complete active space self-consistent field (CAS-SCF) calculations [27] covering an active reference space as described above, were carried out. In this treatment, the $1s$, $2s$, $2p$, $3s$, $3p$, and $3d$ orbitals of selenium were kept doubly occupied but variationally optimized. In the subsequent MRCI treatment only the six valence electrons of each selenium atom were correlated. Since the truncated CI methodology is not size extensive [28], the multireference analog of the renormalized Davidson correction [29] was applied to achieve approximate size extensivity for the final energies $E_{\mathrm{MRCI}+Q}$:

$$E_{\mathrm{MRCI}+Q}=E_{\mathrm{MRCI}}+\Delta E_c\,\frac{1-c_0^2}{c_0^2}.$$

Here ΔE_c denotes the difference between the MRCI and CAS-SCF energies, and c_0^2 is the weight of the reference space in the total MRCI expansion. Finally, the first-order perturbational estimate for the scalar relativistic correction [30] was obtained from the expectation values of the MRCI wave functions with respect to the mass-velocity and Darwin operators, and added to the MRCI$+Q$ energies to obtain the final energies $E_{\mathrm{MRCI}+Q+R}$. All results presented for the selenium dimer include this relativistic correction. For the various electronic states of Se_2 and Se_2^-, these calculations were performed at 20–30 internuclear distances. The number of reference CSFs, the total lengths of the MRCI expansions and selected total energies are given in Table I. Spectroscopic constants were obtained via analytic expressions fitted (fit error <0.001 a.u.) to the *ab initio* calculated potential-energy curves, in which the rovibrational Schrödinger equation for nuclear motion was solved according to Numerov's numerical method. Transition dipole moments for Se_2 and Se_2^- were calculated from CAS-SCF wave functions using the CAS state interaction method [31]. Finally, a brief comment on a more technical point: Due to the use of D_{2h} rather than true $D_{\infty h}$ symmetry in the calculations on the selenium dimer, the two considered $^2\Sigma_u^{+/-}$ states transform in the same irreducible representations (B_{1u} and A_u) as the two degenerate components of the $^2\Delta_u$ state. For these states, the molecular orbitals were optimized in state-averaged CAS-SCF calculations including the two lowest roots, which where subsequently used in individual MRCI calculations on either of the two states. For the $^2\Delta_u$ state, the resulting bond lengths and vibrational frequencies showed only marginal (<0.01 bohr and <2 cm^{-1}) deviations from results obtained with single-root optimized CAS-SCF orbitals, so that we are also confident that the errors for the $\Sigma^{+/-}$ states' properties introduced by the use of state-averaged orbitals are negligible with respect to the errors due to other approximations made here. The CAS-SCF/MRCI studies were performed with the MOLCAS-3 software [32] on IBM RS/6000 workstations at TU Berlin.

To assess the importance of higher than double excitations in the treatment of dynamic electron correlation, the coupled-cluster theory [33], including all single and double excitations and a perturbational treatment of the connected triple excitations [CCSD(T)] was used at some points of the Se/Se^- and $Se_2Se_2^-$ calculations. CCSD(T) has the advantage of being strictly size extensive, and thus should yield more reliable results compared to the MRCI method for chemical processes, during which the number of correlated electrons per fragment changes, i.e., electron affinities and binding energies. Thus most of the Se_3/Se_3^- calculations were also performed using CCSD(T). The coupled-cluster calculations were based on spin-restricted Hartree-Fock reference functions using the RCCSD(T) code of MOLPRO94 [34], as installed on CRAY-YMP computers of the Konrad-Zuse Zentrum für Informationstechnik, Berlin.

Spin-orbit effects were evaluated from CAS-SCF wave functions with the one-electron part of the Breit-Pauli Hamiltonian [35] according to a method described recently [36]. Within the chosen RECP—basis-set description, the effective charge of selenium in the spin-orbit calculations was chosen as $Z_{\mathrm{eff}}=1401$, thus reproducing the experimental $^2P_{3/2}$-$^2P_{1/2}$ splitting of the atomic Se^- ground state (2270 cm^{-1} [10(a)]) quantitatively at the CAS-SCF level of theory. The program system GAMESS [37], installed on an IBM RS/6000 workstation, was used for these calculations.

III. RESULTS AND DISCUSSION

A. Atomic properties of selenium

To investigate the suitability of the computational strategy employed, we first focus on the electron affinity of the selenium atom, for which the experimental value (corrected for spin-orbit splitting, which was not included in the calculations discussed here) amounts to 2.044 eV [10]. Calculated EA's at various levels of theory and using different ANO contractions [38] are given in Table II. First consider the calculations without corrections for relativistic effects: Not surprisingly, the calculated value at the Hartree-Fock level (1.001 eV using the 765 321 ANO set [39]) is less than 50% of the experimental figure due to the neglect of dynamic electron correlation. Treating these effects in the valence shell within the CI method corrected for size-extensivity (CISD$+Q$ in the present case due to the single-reference character of Se and Se^-) increases the theoretical EA to 1.984 eV in the uncontracted $22s17p12d4f3g$ basis set. The 76532 ANO contraction, which constitutes the $spdfg$ part of the basis used for the *molecular* calculations, yields an EA only 0.004 eV lower compared to the uncontracted basis set. Thus the basis set contraction scheme employed here should be well suited for the description of both atomic Se^- and anionic Se_n^- molecules.

TABLE I. Selected total MRCI+Q+R energies for ground and excited states of Se_2 and Se_2^- (in hartree).

			Se_2		
R (bohr)	$X\ ^3\Sigma_g^-$	$a\ ^1\Delta_g$	$b\ ^1\Sigma_g^+$	$A\ ^3\Pi_u$	$B\ ^3\Sigma_u^-$
			Energies		
3.70	−4855.127 68	−4855.106 96	−4855.091 54	−4854.961 42	−4854.960 11
4.00	−4855.153 86	−4855.134 71	−4855.121 18	−4855.008 59	−4855.012 91
4.20	−4855.155 03	−4855.137 12	−4855.125 09	−4855.027 58	−4855.031 55
4.40	−4855.148 74	−4855.132 24	−4855.121 82	−4855.038 68	−4855.040 60
4.60	−4855.138 09	−4855.123 13	−4855.114 30	−4855.044 30	−4855.043 36
4.80	−4855.125 16	−4855.111 88	−4855.105 66	−4855.046 19	−4855.042 05
5.00	−4855.111 34	−4855.099 87	−4855.094 33	−4855.045 66	−4855.038 26
5.20	−4855.097 55	−4855.088 12	−4855.083 77	−4855.043 72	−4855.033 04
5.40	−4855.084 52	−4855.077 07	−4855.074 00	−4855.041 13	−4855.027 18
5.60	−4855.072 49	−4855.067 10	−4855.065 51	−4855.038 47	−4855.021 00
6.00	−4855.052 87	−4855.051 38	−4855.052 27	−4855.036 17	−4855.009 46
50.00	−4855.026 53				−4854.987 82
CSFs[a]	48	36	60	48	48
	5 665 388	3 207 560	4 161 156	6 317 164	5 665 388

			Se_2^-			
R (bohr)	$X\ ^2\Pi_g$	$a\ ^4\Sigma_u^-$	$A\ ^2\Pi_u$	$B\ ^2\Delta_u$	$C\ ^2\Sigma_u^-$	$D\ ^2\Sigma_u^+$
			Energies			
3.70	−4855.163 63	−4855.066 81	−4855.017 42	−4855.053 90	−4855.067 61	−4855.038 08
4.00	−4855.204 96	−4855.120 25	−4855.091 71	−4855.095 15	−4855.104 95	−4855.081 75
4.20	−4855.215 26	−4855.137 04	−4855.118 25	−4855.112 63	−4855.117 81	−4855.101 52
4.40	−4855.217 18	−4855.147 83	−4855.134 80	−4855.124 36	−4855.125 88	−4855.112 98
4.60	−4855.213 78	−4855.154 39	−4855.143 98	−4855.131 24	−4855.130 59	−4855.121 91
4.80	−4855.207 13	−4855.157 73	−4855.148 13	−4855.136 81	−4855.133 01	−4855.127 82
5.00	−4855.198 67	−4855.158 65	−4855.148 90	−4855.138 36	−4855.133 52	−4855.131 44
5.20	−4855.189 36	−4855.157 84	−4855.147 47	−4855.138 84	−4855.132 58	−4855.133 22
5.40	−4855.179 86	−4855.155 77	−4855.144 65	−4855.138 11	−4855.130 77	−4855.133 69
5.60	−4855.170 64	−4855.153 06	−4855.141 03	−4855.136 56	−4855.128 22	−4855.133 21
6.00	−4855.153 71	−4855.146 40	−4855.132 88	−4855.132 05	−4855.122 20	−4855.130 38
50.00	−4855.097 88					
CSFs[a]	21	8	21	16	16	26
	2 931 263	2 091 928	2 931 263	2 389 953	1 289 953	3 410 032

[a]Number of reference CSFs and total length of the MRCI expansion, respectively.

As pointed out earlier for the sulfur atom [7], it is mandatory to include higher angular momentum functions in the basis set and to extend the treatment of electron correlation in order to increase the accuracy of the calculated EA's. Thus a single h-type function was optimized in conjunction with the 76 532 ANO contraction so as to maximize the calculated EA for the selenium atom at the CISD+Q level. We find that the optimum exponent α_h amounts to 0.45, thus yielding values of 1.997 and 2.057 eV on the CISD+Q and CCSD(T) levels, respectively, the latter with a contribution of 0.078 eV from the perturbational treatment of the triple excitations. The additional higher than double excitations from the Hartree-Fock reference function included in the CCSD(T) compared to the CISD+Q calculations have a very similar influence (+0.06 eV) on the computed EA as in the case of the sulfur atom (+0.08 eV [7]). Finally, if a single i function (α_i=0.6) is added to the 765 321 basis, the EA at the CCSD(T) level amounts to 2.063 eV, if only the valence electrons are correlated. Thus the best directly computed electron affinity for the selenium atom surprisingly [2] *overestimates* the experimental value. It follows that corrections should be applied for the approximations made so far, in particular (i) the neglect of relativistic effects (spin-orbit corrections are already included in the experimental reference EA of 2.044 eV), and (ii) core-core and core-valence correlation effects. Both should actually *decrease* the calculated EA's.

(i) In first-order perturbation theory, the scalar relativistic correction amounts to −0.041 eV at the CISD+Q level using the uncontracted primitive basis. Almost the same result is obtained for the 87 643 (−0.039 eV) and 76 532 (−0.041 eV) ANO contractions. Note, however, that the magnitude of the scalar relativistic correction starts to oscillate with smaller contraction sizes (65 421: −0.019 eV; 54 321: −0.084 eV), an unpleasant feature of the first-order perturbational estimate. However, with sufficient flexibility in the basis set, it appears safe to conclude that the mass-velocity

TABLE II. Calculated electron affinities (EAs) for the selenium atom (in eV).

Method/ANO contraction [38]	EA (nonrelativistic)	EA (relativistic[a])
RHF/765321	1.001	0.948
Valence-only correlation		
CISD+Q/uncontracted[b]	1.984	1.943
CISD+Q/54 321	1.956	1.872
CISD+Q/65 421	1.979	1.960
CISD+Q/76 532	1.980	1.939
CISD+Q/87 643	1.984	1.945
CISD+Q/765 321	1.997	1.956
CCSD/765 321	1.979	
CCSD(T)/765 321	2.057	
CCSD/7 653 211[c]	1.984	
CCSD(T)/765 3211[c]	2.063	
Valence+3s3p3d correlation		
CISD+Q/54 321+33 333	1.803	1.740
CISD+Q/76 532+33 333	1.822	1.773
CISD+Q/87 643+33 333	1.824	1.773
CCSD/765 321+33 333	1.974	
CCSD/7 653 211+33 333[c]	1.980	
Expt.[d]	2.044	

[a]Including scalar contributions (see text).
[b]Full primitive 22s17p12d4f3g set.
[c]i exponent: 0.6 [optimized for the EA at the CCSD(T) level].
[d]From the weighted averages over the J levels of Se(^3P) and Se$^-$(^2P) [10].

and Darwin operators yield a diminishing contribution of about 0.041 eV to the electron affinity of the selenium atom.

(ii) Including the 18 additional 3s, 3p, and 3d electrons in the correlation treatment (using the extended basis set [23]) affects the calculated EA's only marginally at the size-extensive CCSD level, i.e., by -0.004 and -0.005 eV with the 7 654 321 and 7 653 211 contractions, respectively (computation of the perturbative estimate of the triple excitations was not possible for technical reasons). However, even after application of the $+Q$ correction, the CISD EA's with inclusion of single and double excitations from the 3s-3d shells are significantly (about 0.15 eV) lower compared to the valence-only values, thus reflecting the principally missing size extensivity of the CI approach. Note, however, that for the larger ANO contractions the scalar relativistic correction to the EA's remains virtually unaffected by the more extensive correlation treatment.

Thus the best theoretical estimate for the electron affinity of the selenium atom is obtained by adding the scalar relativistic (-0.041 eV) and core-valence correlation (-0.004 eV) corrections to the CCSD(T)-7 653 211 result to obtain a value of 2.018 eV, which is only 0.026 eV lower than the experimental value, and has ''chemical accuracy'' like the similarly computed EA of the sulfur atom [7]. In light of the test calculations, the final small error with respect to the experimental result is attributed to remaining deficiencies in the one- and n-particle space treatments. However, even in slightly smaller ANO contractions and neglecting core correlation, the computed EA's at the CCSD(T) level are in very good agreement with experiment, which provides confidence that *molecular* electron affinities of small selenium clusters (for which our hardware capabilities do not allow calculations including core correlation) also can be reliably computed with this approach.

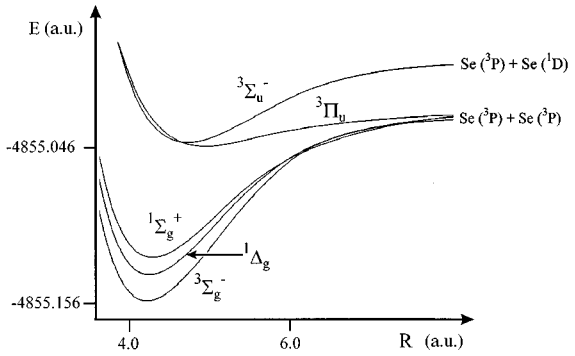

FIG. 1. MRCI+Q potential-energy curves for ground and excited states of Se_2.

As a further test of the quality of the ANO basis set, the atomic dipole polarizability α of the selenium atom was investigated. At the restricted open-shell Hartree-Fock (ROHF) and CISD+Q levels, M_L-averaged values of 25.01 and 25.54 a.u. were obtained with the 765 321 ANO contraction with first-order relativistic corrections $<1\%$. The correlated result shows excellent agreement with the value recommended by Miller for the atomic dipole polarizability of selenium ($\alpha=25.43$ a.u. [40]), while the uncorrelated figure is slightly smaller than the Hartree-Fock results ($\alpha=25.23 \pm 0.05$ a.u.) reported by Sadlej [41] for a ''first-order polarized'' basis set, which has been particularly designed for the description of electric properties. Finally, we have also calculated the dipole polarizabilities for the ^2P ground state of Se^-. This quantity amounts to 50.11 and 53.71 a.u., respectively, at the ROHF and CISD+Q levels with the 765 321 ANO contraction. Compared to the neutral atom, the larger absolute value of the dipole polarizability in the atomic anion reflects its more diffuse charge distribution, while the more significant correlation contribution to α (6.7% compared to 2.0% for Se) is consistent with the large influence of correlation effects on the electron affinity itself.

B. Ground and excited states of neutral Se_2

Since neutral Se_2 is regarded here as a test case for calibration purposes, we restrict ourselves mainly to the spectroscopic properties of those low-lying bound electronic states, for which experimental data have been reported in the literature. The calculated MRCI potential energy curves for its $X\ ^3\Sigma_g^-$, $a\ ^1\Delta_g$, $b\ ^1\Sigma_g^+$, $A\ ^3\Pi_u$, and $B\ ^3\Sigma_u^-$ states are shown in Fig. 1. Corresponding spectroscopic constants are summarized in Table III. While states X, a, b, and A derive from the asymptote with both selenium atoms in their lowest ^3P terms, the $B\ ^3\Sigma_u^-$ state correlates with one ground state ^3P and one excited ^1D term of the Se atom. The X-B system corresponds to the most intense absorption band of the ground-state Se_2 molecule, analogous to the ''Schumann-Runge'' system in O_2. As for Se_2^- (see Sec. III C) the potential-energy curves are based on the data from Table I, thus including the scalar relativistic corrections, but no spin-

TABLE III. Spectroscopic constants (experimental values[a,b] in parentheses) for ground and excited states of Se_2 based on MRCI potential-energy curves.

State	$X\ ^3\Sigma_g^-$ [c]	$a\ ^1\Delta_g$ [d]	$b\ ^1\Sigma_g^+$	$A\ ^3\Pi_u$	$B\ ^3\Sigma_u^-$ [b]
R_e (bohr)	4.122 (4.089)	4.151	4.191 (4.145)	4.845 (4.778)	4.626 (4.616)
$10^3\ B_e$ (cm^{-1})	88.6 (90.1)	87.4	85.7 (87.7)	64.3 (66.0)	70.5 (70.8)
ω_e (cm^{-1})	386 (387)	366	345 (355)	193 (191)	252 (246)
$\omega_e x_e$ (cm^{-1})	1.04 (0.97)	1.02	1.16 (1.10)	2.50 (2.23)	1.06 (1.17)
T_e (cm^{-1})[e]	0.00 (0.00)[f]	4618	7934 (7957)	23829 (24 158)[g]	24822 (25 980)[h]

[a]From Ref. [43].

[b]Experimental values for R_e, B_e, ω_e, and $\omega_e x_e$ are weighted averages over Ω components.

[c]CCSD(T) results: R_e=4.113 bohr; $10^3\ B_e$=89.2 cm^{-1}; ω_e=389 cm^{-1}.

[d]Single root optimized in B_{1g} symmetry.

[e]Excitation energies are with respect to the 0_g^+ component of the ground $X\ ^3\Sigma_g^-$ state and including spin-orbit corrections (see text).

[f]The 1_g component of the $X\ ^3\Sigma_g^-$ state lies 633 cm^{-1} higher in energy than the 0_g^+ component at R=4.666 bohr (expt. T_e: 512 cm^{-1}).

[g]For the 0_u^+ component. The 0_u^-, 1_u, and 2_u components of the A state lie 485, 1000, and 1697 cm^{-1} higher in energy than the 0_u^+ component at R=4.666 bohr (expt. $0_u^+ - 1_u$ T_e value: 772 cm^{-1}).

[h]To the 0_u^+ component. The 1_u component of the B state lies 335 cm^{-1} higher in energy than the 0_u^+ component at R=4.666 bohr (expt. T_e: 80 cm^{-1}).

orbit terms. However, spin-orbit effects, obtained from a diagonalization of the spin-orbit operator H_{SO} within the low-lying state manifold [17,42] {$X\ ^3\Sigma_g^-$, $a\ ^1\Delta_g$, $b\ ^1\Sigma_g^+$, $^3\Delta_u$, $^3\Sigma_u^+$, $A\ ^3\Pi_u$, $B\ ^3\Sigma_u^-$, and $^3\Pi_g$} at R=4.666 bohr (the average bond length for these states according to earlier calculations [17(a)]), are included in the calculated electronic excitation energies T_e. The magnitude for these spin-orbit corrections to T_e lies between 200 and 600 cm^{-1}. As reflected in the experimentally determined spectroscopic data for the individual spin-orbit components of the X, A, and B states [43], spin-orbit coupling influences the other spectroscopic constants of Se_2 only to a small extent (e.g., by 0.004 bohr in the equilibrium bond distance R_e and 1.8 cm^{-1} in the vibrational parameter ω_e for the X state) compared to possible errors introduced by other approximations made in the electronic structure calculations. Thus for the comparison between the experimental and theoretical data, spin-orbit corrections should be more significant for the excitation energies as compared to properties related to first (i.e., bond lengths) or higher (frequencies, anharmonicities) derivatives of the energy.

Before we discuss the quality of the calculations, let us remark that the calculated asymptotic value for the ^3P-^1D separation of selenium (8491 cm^{-1}) is in excellent agreement with the (j-level-averaged) experimental value of 8581 cm^{-1} [10(b)]. Thus it is expected that the molecular excitation energies are also calculated reliably. For the $X\ ^3\Sigma_g^-$ ground state, there is generally good agreement between the calculated MRCI and the experimentally deduced [43] spectroscopic constants: Although the Se-Se equilibrium distance is somewhat overestimated (0.031 bohr, an observation similar to our recent work on S_2 [7]), there are only very small deviations of 1 and 0.07 cm^{-1}, respectively, for the vibrational parameters ω_e and $\omega_e x_e$. Using the CCSD(T) method (with the MRCI scalar relativistic corrections added) the error in the Se-Se bond length is reduced to 0.019 bohr, but for the frequency ω_e it increases to 3 cm^{-1}. The contraction of the Se-Se bond distance is due to the more extensive treatment of dynamic electron correlation on the CCSD(T) level of theory. Notwithstanding the small differences, the similarity between the MRCI and CCSD(T) results provides confidence that the high quality of the calculated spectroscopic parameters does not benefit from fortuitous error cancellation.

Slightly less satisfactory agreement between calculated and experimental results has to be noted for the excited $b\ ^1\Sigma_g^+$, $A\ ^3\Pi_u$, and $B\ ^3\Sigma_u^-$ states. Their bond lengths are overestimated by 0.046 (b), 0.067 (A), and 0.010 (B) bohr. Also, the errors in the frequencies ω_e are somewhat larger compared to the ground state (i.e., 10, 2, and 6 cm^{-1} for states b, A, and B). On the other hand, the spin-orbit-corrected excitation energies for the X-b and X-A transitions miss the experimental values by only 23 and 329 cm^{-1}. Still, the error in the X-B T_e value is 1158 cm^{-1}. We regard these deviations as reasonable in light of the overall large energetic separation of the states involved. Also, the trends for the other spectroscopic constants are computed reliably, and the absolute errors are within the expected range. Overall, these calibration studies suggest that a conservative error estimate for the quality of our spectroscopic constants predicted by our methods for experimentally unknown states of gaseous selenium dimers is $\pm$0.10 bohr for equilibrium distances, $\pm$15 cm^{-1} for vibrational frequencies, and $\pm$1500 cm^{-1} for adiabatic excitation energies.

Finally, we provide predictions for the $a\ ^1\Delta_g$ state, for which accurate experimental information is not available in the literature. Compared to the levels of theory applied earlier [17], our results certainly represent the most accurate predictions for the spectroscopic constants of this state made so far. The Se-Se equilibrium distance in the a state (R_e=4.151 bohr) is predicted to lie intermediate between the values for the X (R_e=4.122 bohr) and b (R_e=4.191 bohr) states, and the same applies to its vibrational frequency. This trend is in line with the earlier theoretical predictions given in Ref. [17(a)]. However, our R_e value is 0.100 bohr shorter, and our ω_e value 42 cm^{-1} larger than those computed by Balasubramanian [17(a)], consistent with the larger basis sets and more extensive electron correlation treatment employed here. Our calculated excitation energy T_e=4618 cm^{-1} is slightly (400 cm^{-1}) lower than those computed previously

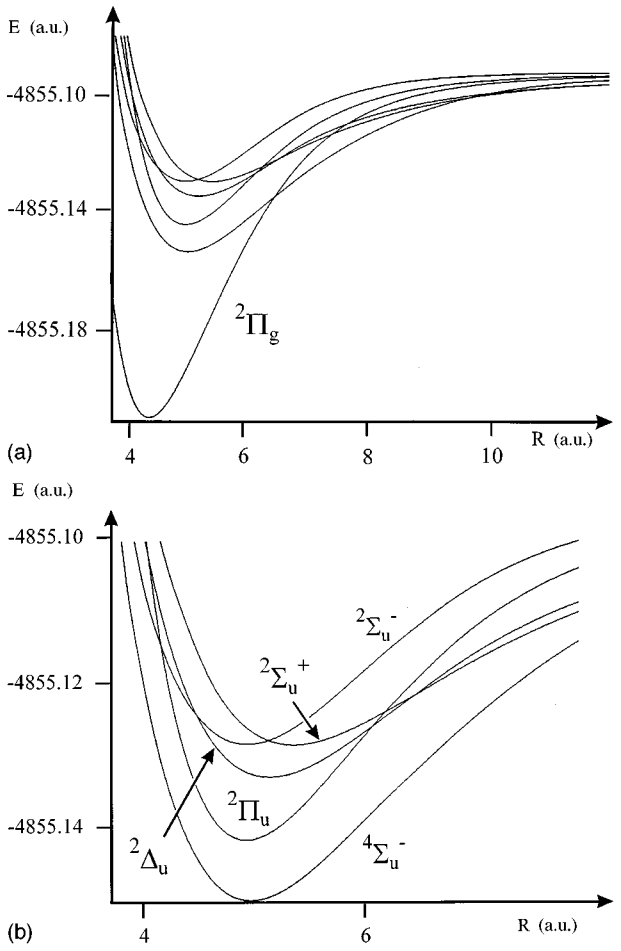

FIG. 2. MRCI+Q potential-energy curves for ground and excited states of Se_2^-: (a) Overview of the electronic spectrum. (b) Close-up of the excited states minimum region.

[17(b),17(c)] nevertheless, these values support an earlier tentative assignment of a feature in the absorption and fluorescence spectra of Se_2 at excitation energies of around 4000 cm^{-1} above the ground state by Yee and Barrow [43]. However, our calculations strongly suggest that the vibrational parameter ω_e=320 cm^{-1} reported by these authors underestimates the true value by about 40–50 cm^{-1}.

C. Ground and excited states of Se_2^-

Potential-energy curves for Se_2^- and corresponding spectroscopic constants are given in Fig. 2 and Table IV, respectively. The qualitative ordering of states as well as the underlying orbital occupation patterns are very similar to the isoelectronic S_2^- molecule [7]: Se_2^- possesses an $X\ ^2\Pi_g$ ground state with a predicted bond distance of 4.358 bohr, 0.236 bohr larger than the equilibrium distance of neutral Se_2 due to the additional electron in an antibonding π_g orbital. The concomitant decrease of the vibrational frequency with respect to the neutral dimer is calculated as 76 cm^{-1}. The spectroscopic constants for the Se_2^- ground state calculated with the CCSD(T) method are again in good agreement to the MRCI results, although the absolute differences (ΔR_e=0.030 bohr, $\Delta\omega_e$=9 cm^{-1}) are somewhat more pronounced than in the neutral. Similar to the S_2^- case [7], the first excited state of Se_2^- is a quartet of $^4\Sigma_u^-$ symmetry. It is predicted to have a significantly longer bond length (R_e=4.994 bohr) than the ground state and also a flatter potential, which is characterized by a frequency at around 170 cm^{-1}. Energetically, the following state is an excited doublet ($^2\Pi_u$ type) with a bond length (R_e=4.957 bohr) very similar to the $^4\Sigma_u^-$, but with a higher vibrational frequency (ω_e=199 cm^{-1}). The higher excited $^2\Delta_u$, $^2\Sigma_u^-$, and $^2\Sigma_u^+$ states are characterized by even longer Se-Se distances and lower vibrational frequencies. Among those states, the largest (smallest) equilibrium distance and the smallest (largest) frequency are predicted for the $^2\Sigma_u^+$ ($^2\Sigma_u^-$) state. The $^2\Delta_u$ spectroscopic properties are intermediate between these two $^2\Sigma$ states. Qualitatively, the excited states' spectrum is very similar to the one calculated for S_2^- [7]: for example, the $^2\Delta_u$-$^2\Sigma_u^-$ crossing occurs at the repulsive wells of the respective potentials, and the $^2\Sigma_u^+$-$^2\Sigma_u^-$ crossing point is located almost vertically above the equilibrium distance of the $^2\Delta_u$ state. However, the S_2^- and Se_2^- electronic spectra differ in the magnitude of the excitation energies: While the manifold of bound states considered here spans 19 500 cm^{-1} (T_e values), the same states of S_2^- lie within about 23 700 cm^{-1}. The remaining two states $^2\Pi_u(II)$ and $^2\Sigma_u^-(II)$ of Se_2^-, which also correlate with the lowest Se^-+Se asymptote, and are connected with the $X\ ^2\Pi_g$ ground state via dipole-allowed transitions, were not included here because they are expected to be repulsive by comparison to S_2^- [7] and O_2^- [12]. For the case of the $^2\Pi_u(II)$ state this assumption was verified by five energy calculations between 3.9 and 5.5 bohr [44]. No indication of a minimum was found. The vertical excitation energies from the Se_2^- ground state to this state at R=4.6 and 5.0 bohr amount to 40 902 and 31 856 cm^{-1}, respectively, at the MRCI level with applied scalar relativistic corrections. For the case of the $^2\Sigma_u^-(II)$ state, a minimum is

TABLE IV. Spectroscopic constants for ground and excited states of Se_2^- based on MRCI potential-energy curves.

State	$X\ ^2\Pi_g$[a]	$a\ ^4\Sigma_u^-$	$A\ ^2\Pi_u$	$B\ ^2\Delta_u$[b]	$C\ ^2\Sigma_u^-$	$D\ ^2\Sigma_u^+$
R_e (bohr)	4.358	4.994	4.957	5.167	4.967	5.385
$10^3\ B_e$ (cm^{-1})	79.3	60.4	61.3	56.4	61.1	51.9
ω_e (cm^{-1})	310	170	199	145	157	127
$\omega_e x_e$ (cm^{-1})	0.985	0.754	0.816	0.549	0.659	0.649
T_e (cm^{-1})[c]	0.00	13 414	15 129	18 097	19 206	19 502

[a]CCSD(T) results: R_e=4.328 bohr; $10^3\ B_e$=80.4 cm^{-1}; ω_e=319 cm^{-1}.

[b]Single root optimized in ^2A_u symmetry.

[c]Including spin-orbit corrections from a diagonalization of H_{SO} in the excited states' manifold {$a\ ^4\Sigma_u^-$, $A\ ^2\Pi_u$, $B\ ^2\Delta_u$, $C\ ^2\Sigma_u^-$, and $D\ ^2\Sigma_u^+$} at R=5.167 bohr, and the fine-structure splitting of the ground state at R=4.358 bohr [$E(^2\Pi_{3/2g})-E(^2\Pi_{1/2g})$=1770 cm^{-1}].

TABLE V. Binding energies[a] for Se_2 and Se_2^- ground states and electron affinities for Se_2 (in eV).

	$Se_2(^3\Sigma_g^-)\rightarrow 2Se(^3P)$	$Se_2^-(^2\Pi_g)\rightarrow Se^-(^2P)+Se(^3P)$	$Se_2^-(^2\Pi_g)\rightarrow Se_2(^3\Sigma_g^-)+e^-$
MRCI+Q	3.35	3.13	1.69
CCSD(T)	3.33	3.24	1.95
Expt.[b]	3.41	3.33±0.07	1.94±0.07

[a]Including calculated spin-orbit corrections.
[b]From Ref. [11].

also unexpected based on the high excitation energy (59 581 cm^{-1} [45]) from the ground state, which exceeds the ground-state well depth by as much as 5 eV.

D. Energetic data for Se_2 and Se_2^-

The calculated bond dissociation energies (BDEs) for neutral and anionic Se_2 as well as adiabatic electron affinities for Se_2 are given in Table V. First of all, it should be noted that with the large one-particle basis sets employed, the basis set superposition error [46] (BSSE) in the present calculations is almost negligible [e.g., at the minimum of the Se_2^- ground state, the BSSE for Se and Se^- at the CCSD(T) level amounts to 0.007 and 0.010 eV, respectively]. The remaining small superposition errors are expected to vanish upon further enlargement of the basis sets employed [47], which will also increase both binding energies and electron affinities. Thus here we compared BSSE-uncorrected theoretical results directly with experiment under the reasonable assumption that at higher levels of theory corrections for basis set superposition and basis set truncation will approximately cancel each other [47].

Consistent with quite similar spectroscopic constants, differences between the BDEs obtained with the MRCI and CCSD(T) methods for both Se_2 and Se_2^- is only small, the MRCI value being slightly (0.02 eV) larger for neutral Se_2 but 0.11 eV smaller for the anion. The higher BDE value obtained with the MRCI method reflects some multiconfigurational character in the Se_2 ground-state wave function, in analogy to S_2 [7]. Similar to our earlier study on the lower homologue [7], the theoretical BDEs for Se_2 are about 0.1 eV lower than the experimental value (3.41 eV [11]). Our result supports the conclusion reached by Drowart and Smoes [48], who found, based on mass-spectrometric experiments, that among two spectroscopic values for the dissociation energy of this species reported earlier [49] (3.17 and 3.41 eV), the lower one was probably in error. The BDE of Se_2^- calculated with the CCSD(T) method is slightly (0.09 eV) higher compared to the corresponding MRCI result due to the more extensive treatment of the n-particle space problem and the single-configuration character of the ground-state wave function near the equilibrium distance. Based on earlier experience with S_2 and S_2^- [7], we expect that the CCSD(T) method underestimates the exact BDE of Se_2^- by about 0.1 eV, which leads to the prediction that the true value is probably in the upper half of the experimentally deduced interval of 3.33±0.07 eV [11].

As for the adiabatic electron affinity of Se_2, the picture is consistent with the results obtained for the EA of the selenium atom in the sense that the CCSD(T) method yields a significantly higher value compared to MRCI (0.26 eV in the present case). Due to the very similar frequencies of the neutral ground state and its anion (Tables III and IV), the zero-point vibrational correction to this quantity is almost negligible (0.01 eV; this correction is included in Table V). The CCSD(T) result (1.95 eV) is found in the upper half of the experimental uncertainty interval (1.94±0.07 eV), suggesting, on the basis of the atomic tests (see above) and earlier experience [7], that the true value for the adiabatic EA of Se_2 is probably slightly larger than 1.94 eV rather than below this value, in accord with the conclusion drawn for the ground-state binding energy of Se_2^-.

E. Radiative lifetime of Se_2 $B\ ^3\Sigma_u^-$

The aim of this section is to investigate the performance of the employed methods with respect to transition-matrix elements of the electronic dipole operator, which are required to assign the absorption spectrum of Se_2^-. To this end, we concentrate on the electronic $X\ ^3\Sigma_g^-$-$B\ ^3\Sigma_u^-$ system in neutral Se_2, which has been well characterized spectroscopically [43,49]. Collision-free lifetimes of the upper state due to a dipole-allowed transition to the ground state were measured by various groups [43,50], and range between 34 and 90 ns. Here we have computed the relevant transition dipole elements, the square of which are proportional to the inverse lifetime of the upper state, as a function of internuclear distance (Table VI). For a theoretical estimate about the lifetime of the upper state, the vibrational contributions (Franck-Condon factors) were included, and the transition probability was weighted over the internuclear distance to account for the delocalization of the upper state's vibrational wave function.

Thus the lifetime of the $B\ ^3\Sigma_u^-$ state via spontaneous emission to the $X\ ^3\Sigma_g^-$ ground state is obtained as 61 ns, being almost independent (variations $<0.1\%$) of the upper state level's vibrational and rotational quantum numbers ($v' \leqslant 5$ and $J \leqslant 5$). In view of the complex perturbations between the Se_2 B state [43], the computed lifetime is in good agreement with the available experimental data. In particular, it is gratifying to note that our calculation corroborates the observation of Martínez *et al.* [50] that for the unperturbed levels, the B state's lifetimes are almost independent of the vibrational and rotational quantum numbers v and J. Note, however, that spin-orbit coupling was not included in the present calculation of radiative lifetimes; however, it is difficult to assess its importance by comparing our ΛS-coupled calculations to experiment because of the spread in the reported experimental values [50]. Thus we can only conclude that the methods employed here are expected to reproduce collision-free radiative lifetimes with an accuracy of about ±50%.

TABLE VI. Transition dipole matrix elements for Se_2 and Se_2^-.

	Geometry	Matrix element[a]
	(a) Se_2	
$\langle X\ ^3\Sigma_g^-\|\mu\|B\ ^3\Sigma_u^-\rangle$[b]	R=4.200 bohr	1.048
	R=4.300 bohr	1.023
	R=4.422 bohr	0.990
	R=4.500 bohr	0.968
	R=4.600 bohr	0.937
	R=4.822 bohr	0.863
	R=4.900 bohr	0.835
	R=5.000 bohr	0.798
	R=5.100 bohr	0.759
	(b) Se_2^-	
$\langle X\ ^2\Pi_g\|\mu\|A\ ^2\Pi_u\rangle$[b]	R=4.837 bohr	0.915
	R=4.877 bohr	0.907
	R=4.917 bohr	0.904
	R=4.957 bohr	0.902
	R=4.997 bohr	0.899
	R=5.037 bohr	0.897
$\langle X\ ^2\Pi_g\|\mu\|A\ ^2\Pi_u^-\rangle$[c]	R=4.367 bohr	0.989
$\langle X\ ^2\Pi_g\|\mu\|B\ ^2\Delta_u\rangle$[c]	R=4.367 bohr	0.182
$\langle X\ ^2\Pi_g\|\mu\|C\ ^2\Sigma_u^-\rangle$[c]	R=4.367 bohr	0.359
$\langle X\ ^2\Pi_g\|\mu\|A\ ^2\Sigma_u^+\rangle$[c]	R=4.367 bohr	0.087

[a]In atomic units (1 a.u.=2.541 D).
[b]From IC-MRCI wave functions.
[c]From CAS-SCF wave functions.

F. Implications for spectroscopic experiments on Se_2^- in solid host matrices

Spectroscopic data from gas-phase measurements are not available for any of the electronically excited states of Se_2^- considered here. The only experimental study of the free Se_2^- species is the photoelectron detachment work of Snodgrass *et al.* [11], from which the adiabatic electron affinity of Se_2^- was deduced (see Sec. III D). However, it has been known for quite some time that Se_2^- anions can be incorporated into polar solid host matrices such as alkali halides [4] (e.g., KI) or zeolithes [5]. The methods of absorption, luminescence, and Raman spectroscopy have been applied to these materials in order to learn about the electronic structure of the guest molecule Se_2^-. The more recent work of Lindner *et al.* [4] was the motivation for the calculations presented here, since there was a need for theoretical reference data in the assignment of the observed spectra. Here we discuss the assignments made earlier in light of our theoretical data. The aim of the exercise is not only to verify or falsify the experimental conclusions, but also an assessment of the effects which the solid hosts matrices exert on the Se_2^- anions embedded into them.

The absorption spectra of Se_2^--doped KI and zeolithes each exhibit one broadband in the blue (20 000 cm^{-1}) and ultraviolet (28 000 cm^{-1}) spectral regions. The more intense blue band was assigned to the $A\ ^2\Pi_u \leftarrow X\ ^2\Pi_g$ process [4,5]. Murata, Kishigami, and Kato [5] assigned the *UV* band to the $B\ ^2\Delta_u \leftarrow X\ ^2\Pi_g$ process on the basis of potential-energy curves calculated for O_2^- [12]. Our calculations support the assignment of the blue absorption band: The $A\ ^2\Pi_u \leftarrow X\ ^2\Pi_g$ vertical excitation energy from the equilibrium geometry of the Se_2^- ground state is computed as 18 600 cm^{-1} (the spin-orbit-corrected value referring to the $^2_{\frac{3}{2}u} \leftarrow {}^2_{\frac{3}{2}g}$ transition), with an expected deviation of 1500 cm^{-1} from the experimental values. For comparison, our calculations underestimated the observed $A\ ^2\Pi_u \leftarrow X\ ^2\Pi_g$ peak position in the analogous S_2^--doped materials by 500 cm^{-1} [7]. The computed vertical excitation energies (including spin-orbit corrections computed according to the method used in Table IV) for the other spin- and dipole-allowed processes are $B\ ^2\Delta_u \leftarrow X\ ^2\Pi_g$: 20 850 cm^{-1}; $C\ ^2\Sigma_u^- \leftarrow X\ ^2\Pi_g$: 19 650 cm^{-1}; and $D\ ^2\Sigma_u^+ \leftarrow X\ ^2\Pi_g$: 24 376 cm^{-1}. The former two processes are also in the order of magnitude of the observed blue absorption band. In fact, the absorption spectra reported by Lindner and co-workers [4] exhibit a weak shoulder on the high-energy tail of the blue absorption band which might be attributed to the $B\ ^2\Delta_u \leftarrow X\ ^2\Pi_g$ and/or $C\ ^2\Sigma_u^- \leftarrow X\ ^2\Pi_g$ systems. However, inspection of the relevant transition dipole matrix elements (Table VI) shows that the respective absorption efficiencies should be much smaller compared to the $A\ ^2\Pi_u \leftarrow X\ ^2\Pi_g$ transition. Thus, although within the expected accuracy of the calculation, contributions from transitions into the excited $^2\Delta_u$ and $^2\Sigma_u^-$ states are likely, our calculations suggest assigning the major origin of the blue absorption band of Se_2^- to the intense $A\ ^2\Pi_u \leftarrow X\ ^2\Pi_g$ absorption, and in this respect we agree with the earlier assignments [4,5].

However, our calculations do *not* support the previous assignment [5] of the *UV* band at 28 000 cm^{-1} to the $B\ ^2\Delta_u \leftarrow X\ ^2\Pi_g$ transition. Under this assumption, the disagreement between experimental and calculated transition energies would amount to as much as 7000 cm^{-1}. Rather, the $B\ ^2\Delta_u \leftarrow X\ ^2\Pi_g$ system is likely to be partly hidden under the intense $A\ ^2\Pi_u \leftarrow X\ ^2\Pi_g$ transition (see above). Still, among the remaining bound Se_2^- doublets, which are connected to the ground state via the dipole operator, there is none which matches the *UV* absorption band within the expected precision. The $^2\Sigma_u^+$ state has a vertical excitation energy (24 376 cm^{-1}), roughly comparable to the maximum of the observed *UV* band (28 000 cm^{-1}). However, the deviation of 3500 cm^{-1} is about a factor of 2 larger than expected. Thus, also in light of the small transition dipole matrix element (Table VI), an assignment of the *UV* band to the $D\ ^2\Sigma_u^+ \leftarrow X\ ^2\Pi_g$ transition is questionable. The second states in $^2\Pi_u$ and $^2\Sigma_u^-$ symmetry can also not be responsible for the *UV* absorption band, since they are purely repulsive and do not support any vibrational levels [44,45]. In the search for other possible states, we computed the vertical excitation energies to all quartet states of ''ungerade'' inversion symmetry, which in the case of strong spin-orbit coupling might give rise to dipole-allowed transitions from the ground state. The respective vertical excitation energies are listed in Table VII. Apart from the low-lying $^4\Sigma_u^-$ state, the remaining quartets have excitation energies >50 000 cm^{-1}, which clearly excludes them for an assignment of the UV band. In addition, the experimental absorption spectra [4,5] show no bands at photon energies <2 eV, which means that the lowest quartet state $^4\Sigma_u^-$ is also not populated in these experiments, despite the spin-orbit interaction of this state with the excited doublet states of ungerade symmetry [51]. Thus doublet-quartet transitions are not observed in the absorption spectra of Se_2^- in solid host matrices. The remaining doublet and quartet

TABLE VII. Vertical excitation energies from ground-state Se_2^- to quartet states of ''ungerade'' inversion symmetry at $R=4.36$ bohr (cm^{-1}).

$X\ ^2\Pi_g \rightarrow {}^4\Sigma_u^-$	15 650
$X\ ^2\Pi_g \rightarrow {}^4\Pi_u(I)$	50 383
$X\ ^2\Pi_g \rightarrow {}^4\Pi_u(II)$	54 142
$X\ ^2\Pi_g \rightarrow {}^4\Sigma_u^-(II)$	56 033
$X\ ^2\Pi_g \rightarrow {}^4\Delta_u$	77 467
$X\ ^2\Pi_g \rightarrow {}^4\Sigma_u^+$	79 101

states correlating with $Se(^3P)+Se^-(^2P)$ are of ''gerade'' symmetry, and dipole transitions into these states from the ground state are forbidden by the fundamental gerade-ungerade parity selection rule. In conclusion, on the basis of our calculations, the UV absorption band at 3.6 eV *cannot be assigned to any electronic transition within the Se_2^- molecule*. Thus, one might speculate that the respective process involves the detachment of the excess electron from the Se_2 molecule into the solid host matrix. However, under this assumption the question arises about which particular resonance effect gives rise to the observed peak shape, since from a purely energetic point of view electron detachment should simply involve an energetic threshold and not the give rise to a profile similar to Franck-Condon-type electronic transitions, as observed experimentally.

A possible solution to this point is to assign the UV band to the intense $X\ ^3\Sigma_g^- \text{-} B\ ^3\Sigma_u^-$ system of the *neutral* Se_2 molecule. The corresponding vertical excitation energy (neglecting spin-orbit coupling) is computed as 27 000 cm^{-1}, in good agreement with the observed UV band maximum. However, the Raman spectra of the selenium-doped materials show no indication of neutral Se_2 at laser excitation energies of 2.4 eV (the 514-nm line of the Ar^+ laser) [4]. Furthermore, Murata, Kishigami, and Kato have shown that an excitation of the samples in 28 000-cm^{-1} absorption band gives rise to $A\ ^2\Pi_u \rightarrow X\ ^2\Pi_g$ luminescence of the Se_2^- anion, which is compatible with the idea that the UV band is an intrinsic property of the Se_2^- molecule. Notwithstanding, this result may also be explained by a sequential mechanism involving primary UV excitation of neutral Se_2, followed by $B\ ^3\Sigma_u^- \rightarrow X\ ^3\Sigma_g^-$ emission (the respective band lies around 20 000 cm^{-1} [4,43], which in turn excites Se_2^- color centers, whose luminescence is subsequently observed. The insensitivity of the Raman measurement to Se_2 possibly present in the solid hosts could be connected with the fact that the chosen excitation energy of 2.4 eV provides the condition of efficient resonant Raman scattering for the $Se_2^-(A\ ^2\Pi_u \leftarrow X\ ^2\Pi_g)$ anion but not for the neutral counterpart. Raman measurements at additional excitation laser wavelengths are required to investigate this possibility. To summarize, the fact that the UV band in the selenium-doped materials [4,5] cannot be assigned to Se_2^- by theory leads to some speculation whether, besides Se_2^-, neutral Se_2 molecules might also possibly be incorporated in the solid host materials. Presently, one can only speculate on this possibility, and additional spectroscopic experiments (e.g., vibrationally resolved absorption measurements) would be helpful to settle the origin of the UV band. An interesting key question here is whether experimental conditions allow for an interconversion between neutral and negatively charged selenium dimers via reversible electron transfer with the host matrices. Also, *ab initio* quantum chemistry is challenged by this question, which calls for an evaluation of the environment effect on the intrinsic electronic properties of the selenium dimers.

After excitation in the 20 000-cm^{-1} band, matrix-embedded Se_2^- molecules exhibit $A\ ^2\Pi_u \rightarrow X\ ^2\Pi_g$ luminescence bands with sharp vibrational progressions, from which ground- and excited-state spectroscopic constants have been derived. The 0-0 lines for these transitions have been observed at 16 011 cm^{-1} in KI and 16 633 cm^{-1} [4] (average values of the series assigned as ''big'' and ''small'') in zeolithes, to which our theoretical prediction (15 073 cm^{-1}, Table IV) agrees within the expected range. The matrix shift of about 600 cm^{-1} between the two different host materials indicates that, for the free species, the theoretical value might be even closer to the experimental one. In this context, note that, with respect to the unperturbed Se_2^- anion, a matrix-induced blueshift of the 0-0 transition is expected since the excited state with the larger equilibrium distance interferes more strongly with the surrounding crystal lattice. The spectroscopic constants of ground state Se_2^- in KI (zeolithes) have been given [4] as $R_e=4.25$ (4.25) bohr, $\omega_e=329$ (334) cm^{-1}, and $\omega_e x_e=0.75$ (0.86) cm^{-1}. The ground-state frequencies were also observed in the Raman spectra at 329 cm^{-1} KI [5]) and 335 or 328 cm^{-1}, respectively (zeolithes [4,52], respectively). The deviations ($\Delta R_e=0.1$ bohr; $\Delta\omega_e=32\pm2$ cm^{-1}, and $\Delta\omega_e x_e=0.16\pm0.06$ cm^{-1}) of these values to our theoretical predictions listed in Table III are larger than for the gaseous neutral Se_2 molecule (see above). We attribute this larger disagreement to compressive solid-state effects of the Se_2^- molecules, as reflected in the equilibrium distances. Based on the ground-state results for neutral Se_2, one can estimate that the solid matrices shorten the ground-state equilibrium distances of Se_2^- by about 0.07 bohr, with a concomitant frequency increase by 10–20 cm^{-1}. The excited $^2\Pi_u$ states' spectroscopic constants have been given as $R_e=4.93$ (4.84) bohr, and $\omega_e=221$ (227) cm^{-1} [4]. Here the deviations from the theoretically predicted values are in the same range as for the ground state. The excited state's R_e value predicted from the luminescence band in KI (4.93 bohr) appears to be somewhat high in light of the results for the ground state.

The $A\ ^2\Pi_u \rightarrow X\ ^2\Pi_g$ luminescence decay in a solid KI matrix at $T=2$ K has been characterized by an inverse time constant of 85 ns by Murata, Kishigami, and Kato [5]. This lifetime was attributed to the lowest ($v'=0$) vibrational level supported by the $A\ ^2\Pi_u$ electronic state due to spontaneous transitions into all possible vibrational levels of the ground state. An additional ''hot luminescence'' from higher vibrational levels of the $A\ ^2\Pi_u$ state into the ground state's vibrational levels was characterized by decay time in the order of 50 ps. Following the procedure outlined for the $B\ ^3\Sigma_u^- \rightarrow X\ ^3\Sigma_g^-$ decay (Sec. III E, Table VI), we calculated the radiative lifetimes of the lowest five vibrational levels supported by the $A\ ^2\Pi_u$ state due to radiative transition into the $X\ ^2\Pi_g$ ground state. The following results were obtained: $\tau(v'=0)=205$ ns, $\tau(v'=1)=202$ ns, $\tau(v'=2)=200$ ns, $\tau(v'=3)=198$ ns, and $\tau(v'=4)=197$ ns. These results are roughly twice as large compared to the measurement of Murata, Kishigami, and Kato ($\tau=85$ ns for the ''ordinary lumi-

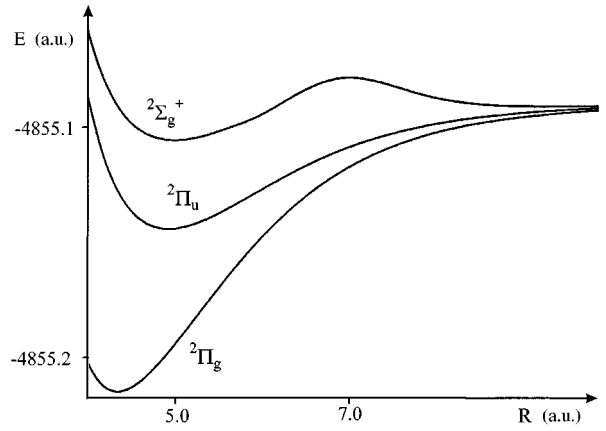

FIG. 3. MRCI+Q potential-energy curves for the $^2\Sigma_g^+$, $A\ ^2\Pi_u$, and $X\ ^2\Pi_g$ states of Se_2^-.

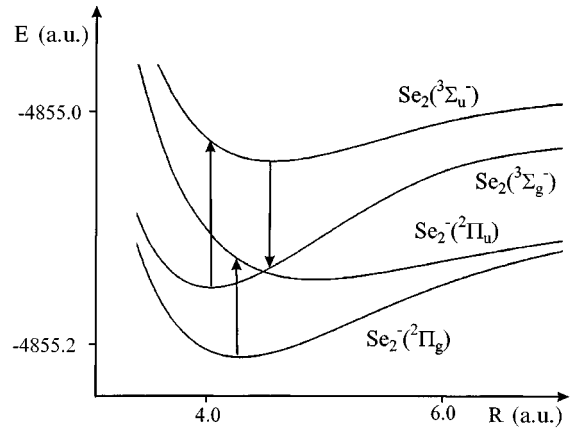

FIG. 4. Two-photon mechanism leading to Se_2 $B\ ^3\Sigma_u^- \rightarrow X\ ^3\Sigma_g^-$ luminescence based on MRCI+Q potential-energy curves.

nescence'' from the $v'=0$ level of the $A\ ^2\Pi_u$ state), a deviation larger than expected on the basis of the radiative lifetime of excited neutral Se_2 (Sec. III E). However, in contrast to the latter case, the experiment on Se_2^- was carried out in a solid environment, which is likely to enhance the transition probabilities due to the additional destabilization of the excited state by a crystal lattice. Thus the measured fluorescence decay dynamics are still in agreement with the theoretical prediction for the $A\ ^2\Pi_u \rightarrow X\ ^2\Pi_g$ system. On the other hand, the calculated dependence of the radiative lifetime on the upper state's vibrational quantum number is rather weak (see above), and does not explain why hot luminescence from higher vibrational levels of the $A\ ^2\Pi_u$ state should proceed with a time constant in the range of 50 ps [5], more than three orders of magnitude faster than the decay of the $v'=0$ vibrational level. Nonradiative decay mechanisms due to interactions with higher-lying states can be ruled out, since vibrational levels with $v'<10$ lie below the minimum of the next higher electronic state, $^2\Delta_u$. The serious disagreement of the fast decay constant with our calculations suggests that the origin of the rapidly decaying fluorescence should be reinvestigated experimentally.

Murata, Kishigami, and Kato [5] also investigated the influence of the temperature (T) on the fluorescence decay dynamics: It was found that both the lifetime of the excited $A\ ^2\Pi_u$ state and its fluorescence intensity-decay exponentially with T. By reference to earlier calculations on O_2^-[12], this was explained in terms of the existence of an additional nonradiative decay pathway for the $A\ ^2\Pi_u$ state via transitions into an excited $^2\Sigma_g^+$ state due to a crossing of the two states near the second vibrational level of $A\ ^2\Pi_u$. To check this hypothesis, we have calculated the potential-energy curve of the $^2\Sigma_g^+$ state, which is displayed in Fig. 3 together with those of the $X\ ^2\Pi_g$ ground and the $A\ ^2\Pi_u$ states. The $^2\Sigma_g^+$ state potential-energy curve exhibits a minimum at $R_e=5.03$ bohr and a local maximum at $R=7.05$ bohr. This potential-energy well (the well depth is 0.72 eV, $T_e=2.80$ eV) supports 19 vibrational levels characterized by the vibrational parameter $\omega_e=168$ cm^{-1}. The particular form of the curve is due to an avoided crossing with a higher excited $^2\Sigma_g^+$ state correlating with the excited $Se(^1D)+Se^-(^2P)$ atomic asymptote. It is clearly recognized that this state does not intersect with the $A\ ^2\Pi_u$ state. Thus nonradiative transitions into this state cannot be the reason for the temperature dependence of the $A\ ^2\Pi_u$ state fluorescence, contrary to the proposal made by Murata, Kishigami, and Kato [5]. We take this example as a justification of our calculations: In spite of the qualitative similarity between the electronic spectra of S_2^- and Se_2^- to the one of O_2^-, quantitatively accurate theoretical data are required for the heavier systems if their physical properties shall be reliably interpreted.

In addition to the Se_2^- $A\ ^2\Pi_u \rightarrow X\ ^2\Pi_g$ band, selenium-doped zeolithes exhibit a second luminescence band, characterized by a 0-0 line at 23 816 cm^{-1} and a lower state vibrational progression of $\omega_e=385$ cm^{-1} [4]. This second ''blue'' emission band was, however, only observed if the wavelength of the excitation laser was in the UV range (about 28 000 cm^{-1}). According to its vibrational fine structure, it must be assigned to the $B\ ^3\Sigma_u^- \rightarrow X\ ^3\Sigma_g^-$ emission of *neutral* Se_2. Under the assumption that the investigated samples contain only anionic Se_2^- color centers (see above), the postulated mechanism [4] for this process involves (i) primary photodetachment of the Se_2^- anion by the UV photon under transfer of an electron onto the solid host matrix (e.g., by reduction of a Na_4^{4+} cluster [4]) followed by (ii) absorption of a second UV photon by the so-generated $X\ ^3\Sigma_g^-$ state of Se_2. The calculated potential-energy curves (Fig. 4) are in agreement with (i) the initial excitation of Se_2^- from the ground state to a higher vibrational level belonging to the excited $A\ ^2\Pi_u$ state, (ii) electron transfer from the excited state to the host matrix under formation of the neutral $Se_2\ ^3\Sigma_g^-$ ground state, (iii) UV excitation of the latter to the excited $B\ ^3\Sigma_u^-$ state by a second photon, and (iv) luminescence to $Se_2\ X\ ^3\Sigma_g^-$. Note that the $^2\Pi_u$ state of Se_2^- crosses the $^3\Sigma_g^-$ state of Se_2 at around $R=4.5$ bohr, between the minima of the two Se_2^- states involved in step (i) such that the excited state's vibronic wave function extends into the crossing region in which the electron transfer process should take place.

G. The Se_3 and Se_3^- clusters

The $^1A_1$ ground-state potential-energy surfaces [16] of neutral X_3 clusters with X=O, S, Se, and Te are known to support two minima, a C_{2v} and a D_{3h} isomer, respectively. These two structures are connected via a C_{2v}-symmetric

TABLE VIII. Optimized geometries and relative energies for the C_{2v} symmetric forms of Se_3 and Se_3^- and the D_{3h} isomer of Se_3 from CCSD(T) calculations.

	$Se_3(C_{2v})$	$Se_3^-(C_{2v})$	$Se_3(D_{3h})$
Geometry	$R_{Se\text{-}Se}$=4.195 bohr θ(Se-Se-Se)=114.8°	$R_{Se\text{-}Se}$=4.317 bohr θ(Se-Se-Se)=113.5°	$R_{Se\text{-}Se}$=4.479 bohr θ(Se-Se-Se)=60.0°
Relative energy (eV)[a]	0.20	−2.38	0.00

[a]Including scalar relativistic corrections.

transition state, which, for the case of O_3, has been characterized as lying close to a conical intersection seam [53]. Both experiments and theory have shown that for X=O and S, the global minimum on this surface corresponds to the C_{2v} isomer [8,14]. For the case of Se_3, earlier theoretical work pointed to a near-accidental degeneracy between the two isomers [15,16,19]. Based on CI calculations in a small basis set, Balasubramanian and Dai predicted that the C_{2v} structure should lie 0.15 eV below the D_{3h} isomer [19(b)]. However, in light of our calibration studies the level of theory employed by these authors cannot be regarded as sufficient for accurate energetic predictions. To this end, we have optimized the geometries for both isomers of Se_3 using the CCSD(T) method (Table VIII). Similar to O_3 and S_3, the Se-Se bond length is found to be smaller in the C_{2v} (4.195 bohr) compared to the D_{3h} isomer (4.479 bohr). The Hartree-Fock wave functions of the C_{2v} and D_{3h} forms have the orbital occupation patterns $(1-21a_1)^2(1-8b_1)^2(1-16b_2)^2(1-6a_2)^2$ and $(1-21a_1)^2(1-9b_1)^2(1-15b_2)^2(1-6a_2)^2$, respectively. Similar to O_3 and S_3 [15,16], there is a second important valence configuration for the C_{2v} form of Se_3, with a weight of 7.4% in the valence CAS-SCF wave function (active space: $4s$ and $4p$ orbitals; weight of the Hartree-Fock configuration: 84.0%). On the other hand, the D_{3h} form is reasonably well described by its Hartree-Fock determinant (91.2% weight in a CAS-SCF as defined above). Accordingly, treating both isomers on an equal basis in order to evaluate their relative energies seems to call for a multireference method. However, as shown in our earlier work on S_3 [8], the CCSD(T) approach yields energy differences between these two isomeric forms which are very close to those obtained with the multireference CI method (mutual deviations $<$0.04 eV), and a similar trend also applies to O_3 [54]. Thus, despite its single-reference character, the CCSD(T) method seems to treat near-degeneracy effects in the C_{2v} form properly. The best theoretical predictions place the C_{2v} forms of ozone and its thioanalog some 1.3 and 0.2 eV, respectively, below the D_{3h} isomers.

In contrast to these lighter homologues, CCSD(T) calculations predict that the D_{3h} isomer corresponds to the global minimum on the ground-state potential-energy surface (PES) of Se_3. At the equilibrium geometry, its relative energy lies 0.20 eV below the optimized C_{2v} structure. At the IC-MRCI+Q level of computation [CCSD(T) geometries], the relative stability of the D_{3h} vs the C_{2v} form is obtained as 0.17 eV, thus corroborating the validity of the single reference CCSD(T) ansatz. Scalar relativistic effects affect this isomeric energy difference by less than 0.01 eV, and zero-point vibrational effects should also be negligible, as noted earlier for O_3 [14(c)]. Considering the C_{2v} vs D_{3h} energy difference for the lighter X_3 clusters (see above), we note that there is a trend of increasing relative stability of the D_{3h} form down the sixth main group of the Periodic Table. Accordingly, the global minimum of Te_3 should also correspond to an equilateral triangle, as predicted earlier by Basch [16]. The validity of this hypothesis and the reasons for the periodic trend will be investigated in the near future [55]. However, it should not remain unmentioned that both Se_3 [56,57] and Te_3 [58] appear to adopt C_{2v} symmetric forms in a solid argon matrix. It is possible that this particular environment favors the C_{2v} isomers over the unpolar D_{3h} forms due to electrostatic and inductive interactions with matrix atoms. Spectroscopic information on the gas-phase structures of Se_3 and Te_3 are required to settle this point.

Furthermore, the Se_3^- anion was studied. As shown earlier [16], this molecule adopts a C_{2v}-symmetry $^2B_1$ ground state arising from the C_{2v} isomer of neutral Se_3 by the addition of one electron in the lowest unoccupied molecular orbital, $9b_1$. With respect to its neutral counterpart, the Se-Se bond length increases by 0.122 bohr, and the Se-Se-Se angle shrinks slightly by 1.3°. For the adiabatic electron affinity, the CCSD(T) results amounts to 2.38 eV (Table VIII), and the vertical detachment energy at the anion equilibrium geometry is computed as 2.71 eV. On the basis of our CCSD(T) studies on O_3/O_3^-, S_3/S_3^- (adiabatic EAs underestimated by 0.06 and 0.07 eV, respectively [8,9(g)]), Se/Se^-, and Se_2/Se_2^- (see above), this result suggests that the true adiabatic electron affinity of Se_3 is probably $>$2.45 eV, thus being significantly larger than the experimentally established lower bound of 2.2 eV [11]. Our calculations indicate that the nonobservation of photoelectron detachment of Se_3^- with 2.54-eV photons is due to a thermodynamic restriction for the single-photon absorption and/or electron detachment mechanism, as suspected by Snodgrass *et al.* [11]

The calculated binding energies of the Se_3 and Se_3^- clusters with respect to Se_2 and an atomic $Se^{0/-}$ fragment are

TABLE IX. Calculated ground-state binding energies for the neutral and anionic Se_3 clusters (in eV).

	$Se_3(^1A_1, D_{3h}) \rightarrow Se_2(^3\Sigma_g^-) + Se(^3P)$	$Se_3^-(^2B_1) \rightarrow Se_2(^3\Sigma_g^-) + Se^-(^2P)$
CCSD(T)[a]	2.01	2.43

[a]Including scalar relavistic terms for all fragments and spin-orbit corrections for the open-shell fragments.

TABLE X. Transition dipole matrix elements (from CAS-SCF wave functions) and vertical excitation energies for low-lying states of Se_3^-.

	Geometry	Matrix element (a.u.)	Vertical transition energy (eV)
$\langle X\ ^2B_1\|\mu\|A\ ^2B_2^-\rangle$	$Se_3^-(^2B_1)$	0.000	1.316 (CAS-SCF[a])
			1.270 (IC-ACPF[b])
			1.263 [CCSD(T)]
$\langle X\ ^2B_1\|\mu\|B\ ^2A_1^-\rangle$	$Se_3^-(^2B_1)$	0.032	1.529 (CAS-SCF[a])
			1.425 (IC-ACPF[b])
			1.412 [CCSD(T)]
$\langle X\ ^2B_1\|\mu\|C\ ^2A_2^-\rangle$	$Se_3^-(^2B_1)$	1.323	1.607 (CAS-SCF[a])
			1.517 (IC-ACPF[b])
			1.557 [CCSD(T)]

[a]State-averaged CAS-SCF with equal weights for the four low-lying states.

[b]Internally contracted multireference averaged coupled pair functional method (size-extensive extension of the MRCI approach, as implemented in MOLPRO94 [34]).

given in Table IX. Spin-orbit effects for the open-shell fragments are included in the values given, but zero-point vibrational energy effects on these binding energies were not explicitly evaluated. However, the latter can be estimated to be smaller than 0.05 eV [7], which makes their contribution small with respect to the overall expected accuracy of these computations. The binding energy of the neutral Se_3 molecule is found to be about 0.4 eV smaller than the one of the Se_3^- anion, in analogy with the trend for S_3/S_3^- [7]. Overall, the bond strengths in the selenium species are about 0.5 eV lower compared to the sulfur analogs, which is in line with the respective trends for the neutral and anionic dimers. Since the heat of formation of neutral Se_3 is not known, our computed binding energies cannot be compared to the experimental data. The accuracy of these predictions is estimated as ± 0.2 eV.

Supplementing earlier information for O_3^- [6] and S_3^- [8], Table X reports the vertical excitation energies and associated dipole matrix elements from the ground state of Se_3^- to the lowest state of each irreducible representation of the C_{2v} point group. Irrespective of the method chosen for the computation of the excitation energies, the qualitative picture is again similar to the lighter homologues: The lowest excited state has $^2B_2$ symmetry but, by symmetry, a vanishing dipole-matrix element with the ground state. Slightly higher in energy are the $^2A_1$ and $^2A_2$ state, and the latter is expected to be preferentially populated in absorption experiments due to its 41-times-larger transition matrix element with the ground state. Finally, we note that the absolute excitation energies to the three lowest excited states of Se_3^- are smaller compared to the respective sulfur (by about 0.5 eV [8]) and oxygen (by about 1 eV [6]) analogs.

H. Summary

Ab initio calculations on small neutral and anionic selenium species have been performed. For these systems, relativistically corrected multireference configuration-interaction and coupled-cluster wave functions expanded in a large Gaussian-type basis set including up to h-type functions yield accurate ground- and excited-state spectroscopic constants and energetic data. A conservative error estimate for the chosen level of theory based on a comparison to an experimentally known system is ± 0.10 bohr for equilibrium distances, ± 15 cm^{-1} for vibrational frequencies, and ± 1500 cm^{-1} for adiabatic excitation energies. At the coupled-cluster level, the computed ground-state energetic data (binding energies, electron affinities) are within 0.1 eV of known experimental data, but these errors can become larger in configuration-interaction calculations with a less extensive treatment of the dynamic correlation energy.

The following predictions are made for experimentally unknown systems: (i) The first excited singlet state of Se_2, $a\ ^1\Delta_g$, is characterized by the spectroscopic constants $R_e=4.151$ bohr, $\omega_e=366$ cm^{-1}, $\omega_e x_e=1.02$ cm^{-1}, and $T_e=4618$ cm^{-1}. (ii) For Se_2^-, there are four bound excited states ($A\ ^2\Pi_u$, $B\ ^2\Delta_u$, $C\ ^2\Sigma_u$, and $D\ ^2\Sigma_u^+$) correlating with the lowest dissociation channel, which can be reached from the ground state via the electronic dipole operator. The associated adiabatic excitation energies lie between 15 000 and 19 000 cm^{-1}. (iii) The lowest excited states of Se_2^- is of quartet multiplicity ($^4\Sigma_g^-$). Qualitatively, the Se_2^- electronic spectrum is similar to O_2^- and S_2^-. In this series, the electronic excitation energies become smaller for the heavier systems. (iv) A D_{3h} equilibrium geometry, about 0.2 eV more stable than the C_{2v} symmetric isomer, is predicted for the neutral Se_3 molecule. (v) The adiabatic electron affinity of Se_3 should lie at around 2.45 eV.

With reference to the spectroscopic properties of selenium-doped zeolithes and potassium iodide, our calculations allow the following conclusions to be drawn: (i) The most intense absorption and emission bands belong to the $^2\Pi_u$-$^2\Pi_g$ system of the Se_2^- anion. (ii) Assignment of the UV absorption band to any Se_2^- electronic transition appears questionable. (iii) The observation of the neutral Se_2 dimer's $^3\Sigma_u^- \rightarrow {}^3\Sigma_g^-$ emission after UV-photon absorption of selenium-doped sodalith is consistent with a two-step mechanism involving initial electron transfer from electronically excited $Se_2^-(^2\Pi_u)$ to the solid host material.

ACKNOWLEDGMENTS

This work was supported by the Fonds der Chemischen Industrie, the Gesellschaft der Freunde der Technischen Uni--versität Berlin. A generous amount of computer time and excellent service (Dr. T. Steinke) was provided by the Konrad-Zuse Zentrum für Informationstechnik, Berlin. C. H. thanks Professor H. Schwarz, TU Berlin, for his continuous support.

[1] E. Illenberger and J. Momigny, *Gaseous Molecular Ions* (Steinkopf, Darmstadt, 1992).

[2] T. Noro, M. Yoshimine, M. Sekiya, and F. Sasaki, Phys. Rev. Lett. **66**, 1157 (1991); R. A. Kendall, T. H. Dunning, and R. J. Harrison, J. Chem. Phys. **96**, 6796 (1992); D. E. Woon and T. H. Dunning, *ibid*. **98**, 1358 (1993).

[3] For reviews, see K. M. Ervin and W. C. Lineberger, in *Advances in Gas Phase Ion Chemistry*, edited by N. G. Adams and L. M. Babcock (JAI Press, Greenwich CT, 1992), Vol. 1; R. B. Metz, S. E. Bradforth, and D. M. Neumark, Adv. Chem. Phys. **81**, 1 (1992); D. M. Neumark (unpublished); S. Wolf, G. Sommerer, S. Rutz, E. Schreiber, T. Leisner, L. Wöste, and R. S. Berry, Phys. Rev. Lett. **74**, 4177 (1995).

[4] Se_2^- in zeolithe-type matrices: (a) G.-G. Lindner, *Berichte aus der Chemie*, Ph.D. thesis, Marburg, 1994 (Verlag Shaker, Aachen, 1994; ISBN 3-8265-0201-9), and literature cited therein; (b) H. Schlaich, G.-G. Lindner, J. Feldmann, D. Reinen, and E. O. Göbel, J. Chem. Phys. (to be published); (c) G.-G. Lindner, K. Witke, and C. Heinemann, Chem. Phys. (to be published).

[5] Se_2^- in potassium iodide matrices: J. Rolfe, J. Chem. Phys. **49**, 4193 (1968); M. Ikezawa and J. Rolfe, *ibid*. **58**, 2024 (1972); L. Rebane and T. Khaldre, Pis'ma Zh. Eksp. Teor. Fiz. **26,** 674 (1977) [JETP Lett. **26**, 515 (1977)]; L. Vella and J. Rolfe, J. Chem. Phys. **61**, 41 (1974); H. Murata, T. Kishigami, and R. Kato, J. Phys. Soc. Jpn. **59**, 506 (1979).

[6] W. Koch, G. Frenking, G. Steffen, D. Reinen, M. Jansen, and W. Assenmacher, J. Chem. Phys. **99**, 1271 (1993).

[7] C. Heinemann, W. Koch, G.-G. Lindner, and D. Reinen, Phys. Rev. A **52**, 1024 (1995).

[8] W. Koch, J. Natterer, and C. Heinemann, J. Chem. Phys. **102**, 6159 (1995).

[9] (a) R. J. Celotta, R. A. Bennett, and J. L. Hall, J. Chem. Phys. **60**, 1740 (1974); (b) S. E. Novick, P. C. Engelking, P. L. Jones, J. H. Futrell, and W. C. Lineberger, *ibid*. **70**, 2652 (1979); (c) D. W. Arnold, C. Xu, E. H. Kim, and D. M. Neumark, *ibid*. **101**, 912 (1994); (d) S. Moran and G. B. Ellison, J. Phys. Chem. **92**, 1794 (1988); (e) M. R. Nimlos and G. B. Ellison, *ibid*. **90**, 2574 (1986); (f) S. Hunsicker, R. O. Jones, and G. Ganteför, J. Chem. Phys. **102**, 5917 (1995).

[10] (a) Atomic electron affinities are taken from H. Hotop and W. C. Lineberger, J. Phys. Chem. Ref. Data **14**, 731 (1985); (b) Spectroscopic data on the neutral Se atom are from C. E. Moore, *Atomic Energy Levels*, Natl. Bur. Stand. Ref. Data Ser., Natl. Bur. Stand. (U.S.) Circ. No. 35 (U.S. GPO, Washington D.C., 1971).

[11] J. T. Snodgrass, J. V. Coe, K. M. McHugh, C. B. Freidhoff, and K. H. Bowen, J. Phys. Chem. **93**, 1249 (1989).

[12] M. Krauss, D. Neumann, A. C. Wahl, G. Das, and W. Zemke, Phys. Rev. A **7**, 69 (1973); G. Das, A. C. Wahl, W. T. Zemke, and W. C. Stwalley, J. Chem. Phys. **68**, 4252 (1978); G. Das, W. T. Zemke, and W. C. Zemke, *ibid*. **72**, 2327 (1980); K. J. Borve and P. E. M. Siegbahn, Theor. Chim. Acta **77**, 409 (1990).

[13] K. A. Peterson, R. C. Mayrhofer, E. L. Sibert III, and T. C. Woods, J. Chem. Phys. **94**, 414 (1991); R. González-Luque, M. Merchán, P. Borowski, and B. O. Ross, Theor. Chim. Acta **86**, 467 (1993); P. Borowski, B. O. Roos, S. C. Racine, T. J. Lee, and S. Carter, J. Chem. Phys. **103**, 266 (1995).

[14] (a) D. Hohl, R. O. Jones, R. Car, and M. Parrinello, J. Chem. Phys. **89**, 6823 (1988); (b) T. Fueno and R. J. Buenker, Theor. Chim. Acta **73**, 123 (1988); (c) J. E. Rice, R. D. Amos, N. C. Handy, T. J. Lee, and H. F. Schaefer, J. Chem. Phys. **85**, 963 (1986); (d) V. G. Zakrzewski and W. von Niessen, Theor. Chim. Acta **88**, 75 (1994).

[15] W. von Niessen, L. S. Cederbaum, and F. Tarantelli, J. Chem. Phys. **91**, 3582 (1989).

[16] H. Basch, Chem. Phys. Lett. **157**, 129 (1989).

[17] (a) K. Balasubramanian, J. Chem. Phys. **91**, 5166 (1987); (b) K. Bhanuprakash, G. Hirsch, and R. J. Buenker, Mol. Phys. **72**, 1185 (1991); (c) For a review of heavy *p*-block dimers, see K. Balasubramanian, Chem. Rev. **90**, 93 (1990).

[18] (a) E. Broclawik and V. H. Smith, Int. J. Quantum Chem. **14**, 395 (1980); (b) D. Hohl, R. O. Jones, R. Car, and M. Parrinello, Chem. Phys. Lett. **139**, 540 (1987).

[19] G. Igel-Mann, H. Stoll, and H. Preuss, Mol. Phys. **80**, 341 (1993); K. Balasubramanian and D. Dai, J. Chem. Phys. **99**, 5239 (1993).

[20] (a) J. Almlöf and P. R. Taylor, J. Chem. Phys. **86**, 4070 (1987); (b) P.-O. Widmark, P.-Å. Malmqvist, and B. O. Roos, Theor. Chim. Acta **77**, 291 (1990).

[21] H. Partridge, J. Chem. Phys. **90**, 1043 (1989).

[22] D. E. Woon, and T. H. Dunning, Jr., J. Chem. Phys. **103**, 4572 (1995).

[23] *s* exponents: 7.267 185, 3.347 055, and 1.541 556; *p* exponents: 4.869 158, 2.112 966, and 0.926 491; *d* exponents: 8.604 73, 3.398 885, and 1.505 216; *f* exponents: 15.728 674, 6.378 035, and 2.584 673; *g* exponents: 14.997 477, 6.339 254, and 2.679526.

[24] The complete Se basis set is available upon request: ibmpow @garm.teokem.lu.se or kochw@argon.chem.tu-berlin.de

[25] W. J. Stevens, M. Krauss, H. Basch, and P. G. Jasien, Can. J. Chem. **70**, 612 (1992).

[26] For a detailed description of the method, see P. E. M. Siegbahn, in *Lecture Notes in Chemistry*, edited by B. O. Roos (Springer, Berlin, 1992), Vol. SP.

[27] B. O. Roos, Adv. Chem. Phys. **69**, 399 (1987); *Lecture Notes in Chemistry* (Ref. [26]).

[28] W. Duch and G. H. F. Diercksen, J. Chem. Phys. **101**, 3018 (1994).

[29] E. R. Davidson, in *The World of Quantum Chemistry*, edited by R. Daudel and B. Pullmann (Reidel, Dordrecht, 1974); S. R. Langhoff, and E. R. Davidson, Int. J. Quantum Chem. **8**, 61

(1974); E. R. Davidson, and D. W. Silver, Chem. Phys. Lett. **52**, 403 (1977).

[30] R. D. Cowan and D. C. Griffin, J. Opt. Soc. Am. **66**, 1010 (1976); R. L. Martin, J. Phys. Chem. **87**, 750 (1983); V. Kellö and A. J. Sadlej, J. Chem. Phys. **93**, 8122 (1990).

[31] P. Å. Malmqvist, and B. O. Roos, Chem. Phys. Lett. **155**, 189 (1989).

[32] MOLCAS-3 is a package of *ab initio* programs written by K. Anderson, M. R. A. Blomberg, M. P. Fülscher, V. Kellö, R. Lindh, P.-A. Malmquist, J. Noga, J. Olsen, B. O. Roos, A. J. Sadlej, P. E. M. Siegbahn, M. Urban, and P.-O. Widmark.

[33] For excellent reviews, see R. J. Bartlett, J. Phys. Chem. **93**, 1697 (1989); R. J. Bartlett, and J. F. Stanton, in *Reviews in Computational Chemistry*, edited by K. B. Lipkowitz (VCH, New York, 1994), Vol. 5; P. R. Taylor, *Lecture Notes on Quantum Chemistry II*, Lecture Notes in Chemistry Vol. 64 (Springer, Berlin, 1995); R. J. Bartlett, in *Modern Electronic Structure Theory*, edited by D. R. Yarkony (World Scientific, Singapore, 1995), Pt. II.

[34] MOLPRO is a package of *ab initio* programs written by H.-J. Werner and P. J. Knowles, with contributions from J. Almlöf, R. D. Amos, M. J. O. Deegan, S. T. Elbert, C. Hampel, W. Meyer, K. Peterson, R. Pitzer, A. J. Stone, and P. R. Taylor. The open-shell coupled-cluster part of MOLPRO is described in P. J. Knowles, C. Hampel, and H.-J. Werner, J. Phys. Chem. **99**, 5219 (1993).

[35] T. E. H. Walker, and W. G. Richards, J. Chem. Phys. **52**, 1311 (1970).

[36] S. Koseki, M. W. Schmidt, and M. S. Gordon, J. Phys. Chem. **96**, 10 768 (1992); S. Koseki, M. S. Gordon, M. W. Schmidt, and N. Matsunaga, *ibid.* **99**, 12 764 (1995). For an application of this method to transition-metal elements, see C. Heinemann, W. Koch, and H. Schwarz, Chem. Phys. Lett. **245**, 509 (1995).

[37] M. W. Schmidt, K. K. Baldridge, J. A. Boatz, J. H. Jensen, S. Koseki, M. S. Gordon, K. A. Nguyen, T. L. Windus, and S. T. Elbert, QCPE Bull. **10**, 52 (1990).

[38] We use the notation ''*abcde*'' for a contracted basis set of (a) *s* functions, (b) *p* functions, (c) *d* functions, (d) *f* functions, etc.

[39] In the totally uncontracted $23s17p10d6f4g$ primitive basis set, the calculated electron energy for selenium at the Hartree-Fock level is identical to the respective value obtained with the 765 321 ANO contraction.

[40] T. M. Miller, in *CRC Handbook of Chemistry and Physics*, 68th ed. edited by R. C. Weast (Chemical Rubber Co., Boca Raton, FL, 1987).

[41] A. J. Sadlej, Theor. Chim. Acta **81**, 45 (1991).

[42] State-averaged CAS-SCF wave functions (eight active orbitals for the 12 valence electrons), optimized separately for singlets and triplets, with equal weights for each state, were used for the spin-orbit calculations.

[43] S. J. Prosser, R. F. Barrow, C. Effantin, J. d'Incan, and J. Vergès, J. Phys. B **15**, 4151 (1982). For earlier spectroscopic investigations on Se_2 see K. K. Yee and R. F. Barrow, J. Chem. Soc. Faraday Trans. II **68**, 1181 (1972); R. Winter, I. Barnes, E. H. Fink, J. Wildt, and F. Zabel, Chem. Phys. Lett. **73**, 297 (1980); V. E. Bondybey and J. H. English, J. Chem. Phys. **72**, 6479 (1980). A compilation of earlier data is found in K. P. Huber and G. Herzberg, *Molecular Spectra and Molecular Structure IV, Constants of Diatomic Molecules* (van Nostrand Reinhold, New York, 1979).

[44] Total MRCl+Q energies, corrected for scalar relativistic effects: $R=3.90$ bohr, $E=-4854.937\,98$ hartree; $R=4.30$ bohr, $E=-4854.999\,70$ hartree; $R=4.60$ bohr, $E=-4855.027\,43$ hartree; $R=5.00$ bohr, $E=-4855.053\,53$ hartree; $R=5.50$ bohr, $E=-4855.069\,86$ hartree.

[45] MRCI+Q energy corrected for scalar relativistic effects, for $^2\Sigma_u^-$ at $R=4.36$ bohr, $E=-4854.945\,849$ hartree, which lies *above* the lowest dissociation channel.

[46] Estimated by the counterpoise method: S. F. Boys and F. Bernardi, Mol. Phys. **19**, 553 (1970).

[47] P. R. Taylor, in *Modern Electronic Structure Theory*, edited by D. R. Yarkony (World Scientific, Singapore, 1995), Pt. II.

[48] J. Drowart and S. Smoes, J. Chem. Soc. Faraday Trans. II **73**, 1755 (1977).

[49] R. F. Barrow, G. G. Chandler, and C. B. Meyer, Philos. Trans. A **260**, 395 (1966).

[50] G. Gouedard and J. C. Lehmann, C.R. Acad. Sci. (Paris) **280**, B471 (1975); A. V. Stolyarov, N. E. Kuz'menko, Ya. A. Harya, and R. S. Ferber, J. Mol. Spectrosc. **137**, 251 (1989); E. Martínez, F. J. Basterrechea, P. Puyuelo, and F. Castaño, Chem. Phys. Lett. **236**, 83 (1995).

[51] The respective spin-orbit matrix elements (cm^{-1}): $\langle {}^4\Sigma_u^-|H_{SO}|^2\Pi_u\rangle = 374+202i(\Omega=\frac{3}{2})$; $\langle {}^4\Sigma_u^-|H_{SO}|^2\Pi_u\rangle = 216+117i(\Omega=\frac{1}{2})$; $\langle {}^4\Sigma_u^-|H_{SO}|^2\Sigma_u^+\rangle = 1396(\Omega=\frac{1}{2})$.

[52] A. Goldbach, L. Iton, M. Grimsditch, and M.-L. Saboungi, J. Am. Chem. Soc. **118**, 2004 (1996).

[53] (a) S. S. Xantheas, G. J. Atchity, S. T. Elbert, and K. Ruedenberg, J. Chem. Phys. **94**, 8054 (1991); (b) G. J. Atchity and K. Ruedenberg, *ibid.* **99**, 3790 (1993); (c) K. Ruedenberg and G. J. Atchity, *ibid.* **99**, 3799 (1993).

[54] The D_{3h} from of O_3 [$R_{O\text{-}O}=2.778$ bohr, Ref. [53(a)]] is less stable than the C_{2v} isomer [$R_{O\text{-}O}=\theta$ (O-O-O) Ref. [53(a)]] by 1.27 and 1.34 eV on the CCSD(T) and ICMRCI+Q levels of theory with the 6532 ANO contraction used in Ref. [6].

[55] C. Heinemann and W. Koch, work on Te_n/Te_n^- ($n=2$ and 3), presently in progress.

[56] H. Schnöckel, H. J. Gocke, and R. Elsper, Z. Anorg. Allg. Chem. **494**, 78 (1982).

[57] G. D. Brabson, L. Andrews, J. Phys. Chem. **96**, 9172 (1992).

[58] H. Schnöckel, Z. Anorg. Allg. Chem. **510**, 72 (1984).